



Title	Formation and characterization of porous InP layers in KOH Solutions
Author(s)	O'Dwyer, Colm; Buckley, D. Noel; Cunnane, V. J.; Sutton, David; Serantoni, M.; Newcomb, Simon B.
Publication date	2002-10
Original citation	O'Dwyer, C., Buckley, D. N., Cunnane, V. J., Sutton, D., Serantoni, M. and Newcomb, S. B. (2002) 'Formation and Characterization of Porous InP Layers in KOH Solutions', State-of-the-Art Program on Compound Semiconductors XXXVII (SOTAPOCS XXXVII) / Narrow Bandgap Optoelectronic Materials and Devices, 202nd ECS Meeting, Salt Lake City, Utah, 20-24 October, in Proceedings - Electrochemical Society, Vol. 14, pp. 259-269. ISBN 1-56677-306-5.
Type of publication	Conference item
Link to publisher's version	http://ecsdl.org/site/misc/proceedings_volumes.xhtml Access to the full text of the published version may require a subscription.
Rights	© 2002, Electrochemical Society
Item downloaded from	http://hdl.handle.net/10468/2879

Downloaded on 2017-02-12T09:31:40Z

FORMATION AND CHARACTERIZATION OF POROUS InP LAYERS IN KOH SOLUTIONS

C. O'Dwyer^{†‡}, D. N. Buckley^{†‡}, V. J. Cunnane^{†*}, D. Sutton[‡],
M. Serantoni[‡] and S. B. Newcomb[‡]

[†] *Dept. of Physics, University of Limerick, Ireland*

[‡] *Materials and Surface Science Institute, University of Limerick, Ireland*

^{*} *Dept. of Chemistry and Environmental Science, University of Limerick, Ireland*

ABSTRACT

Porous InP layers were formed electrochemically on (100) oriented n-InP substrates in various concentrations of aqueous KOH under dark conditions. In KOH concentrations from 2 mol dm⁻³ to 5 mol dm⁻³, a porous layer is obtained underneath a dense near-surface layer. The pores within the porous layer appear to propagate from holes through the near-surface layer. Transmission electron microscopy studies of the porous layers formed under both potentiodynamic and potentiostatic conditions show that both the thickness of the porous layer and the mean pore diameter decrease with increasing KOH concentration. The degree of porosity, estimated to be 65%, was found to remain relatively constant for all the porous layers studied.

INTRODUCTION

There is presently considerable interest in porous semiconductors and their applications [1-7]. The three-dimensional microstructuring of III-V compounds has been the subject of several recent studies [8,9]. Pore formation on Ge [10], InP [11], GaAs [12], GaP [13,14], and SiC [15] has been studied during potentiostatic or galvanostatic anodisation in acidic solution. The pronounced anisotropy of these compounds with respect to etching [16] makes them potential candidates for the formation of photonic crystals, particularly if ordered arrays of parallel pores can be created. Anion type and concentration can play a significant role in affecting the pore growth and morphology [17,18]. The depth of porous layers and their preferential crystallographic growth directions have been shown to be affected by the substrate type [19], orientation [20] and doping density [21].

This paper presents results of an investigation of the anodic etching of InP in high concentrations of KOH in aqueous solution. The anodic processes were investigated using cyclic voltammetry and the resulting porous structures were characterized using transmission electron microscopy.

EXPERIMENTAL

The working electrode consisted of polished (100)-oriented monocrystalline sulfur doped n-InP with a carrier concentration of approximately 3×10^{18} cm⁻³. An ohmic contact was made by alloying indium to the InP sample and the contact was isolated from

the electrolyte by means of a suitable varnish. The electrode area was typically 0.2 cm^2 . Anodization was carried out in KOH electrolytes varying in concentration from $2 - 5 \text{ mol dm}^{-3}$. A conventional three electrode configuration was used employing a platinum counter electrode and saturated calomel reference electrode (SCE) to which all potentials are referenced. Prior to immersion in the electrolyte, the working electrode was dipped in a 3:1:1 $\text{H}_2\text{SO}_4:\text{H}_2\text{O}_2:\text{H}_2\text{O}$ etchant and rinsed in deionized water. All of the electrochemical experiments were carried out at room temperature and in the dark.

A CH Instruments Model 650A Electrochemical Workstation interfaced to a Personal Computer (PC) was employed for cell parameter control and for data acquisition. The surfaces and/or cross-sections of the anodized samples were examined using a Nikon Nomarski optical microscope, a Joel JSM 840 scanning electron microscope and a Topometrix atomic force microscope. Cross-sectional slices were thinned to electron transparency using standard focused ion beam milling procedures by means of a FEI 200 FIBSIMS workstation. The transmission electron microscopy (TEM) characterization was performed using a JEOL 2010 TEM operating at 200 kV.

RESULTS AND DISCUSSION

Fig. 1 shows the voltammetric response of an n-InP electrode in a 5 mol dm^{-3} KOH solution. The potential was scanned at a rate of 2.5 mV s^{-1} from 0.0 V to 0.7 V. At potentials less than 0.3 V, very little current flow is observed. However, above 0.35 V, the current density begins to increase rapidly from a value of 1 mA cm^{-2} at 0.35 V to a peak value of 20 mA cm^{-2} at 0.48 V. Above 0.48 V, the current density decreases rapidly, reaching a value of 3 mA cm^{-2} at 0.6 V. Clearly a significant anodic oxidation process occurs above 0.35 V and becomes self-limiting at higher potentials.

Cross-sectional TEM examination of electrodes, which have undergone a potential sweep such as that described for Fig. 1 elucidate the type of process involved during the anodization. Fig. 2 is a bright field through focal TEM of the InP cross-section after a potential sweep from 0.0 V to 0.7 V in 5 mol dm^{-3} KOH. A region, marked (A), extending approximately 650 nm into the InP substrate (B), is clearly modified and appears to be penetrated by a network of pores. However, a thin layer ($\sim 30 \text{ nm}$) close to the surface appears to be unmodified. The manner in which such a porous layer can form by electrochemical oxidation despite the presence of this dense InP layer at the surface is not apparent from Fig. 2. Closer examination by TEM, however, reveals the presence of pores through this dense near-surface layer. This is illustrated in the TEM micrograph in Fig. 3 which shows a cross-section of an electrode which had been subjected to a potential sweep from 0.0 V to 0.7 V at a scan rate of 2.5 mV s^{-1} . It can be observed that the dense, near-surface layer appears to be penetrated at one point by a pore. It is also clear that the texture of the porous layer indicates that the pores emanate from this point in the near-surface layer. This suggests a mechanism by which the porous layer can grow, *i.e.* it appears to be connected to the electrolyte by pores through the near-surface layer.

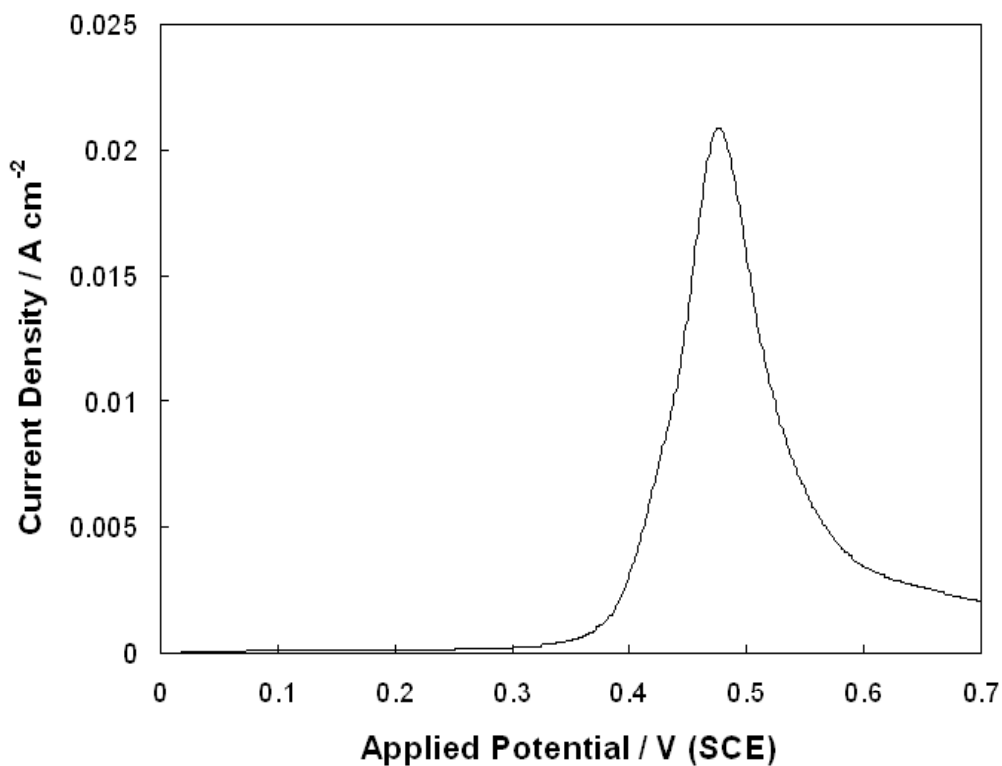


Fig. 1 Linear potential sweep of an n-InP electrode in a 5 mol dm⁻³ KOH electrolyte from 0.0 V to 0.7 V (SCE). The data was acquired at a scan rate of 2.5 mV s⁻¹.

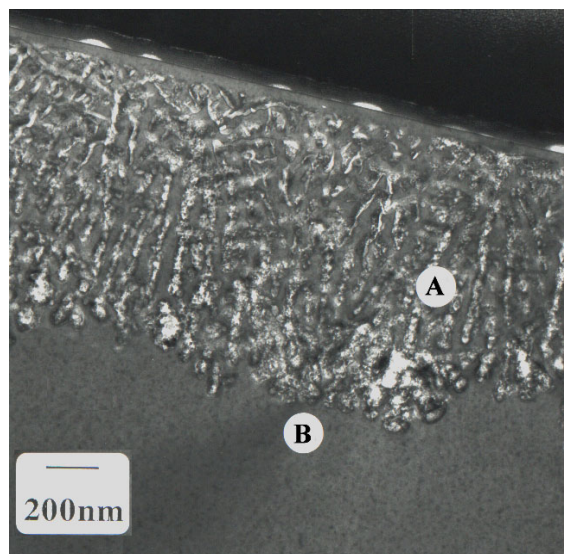


Fig. 2 Cross-sectional bright field through focal TEM of n-InP after a potential sweep from 0.0 V to 0.7 V (SCE) at a scan rate of 2.5 mV s⁻¹ in 5 mol dm⁻³ KOH electrolyte. 'B' denotes the InP substrate. The plane of the micrograph is (110).

Further evidence for the existence of these pores was obtained from AFM measurements of the surface of electrodes. Careful AFM examination of the surface of wafers such as that shown in Fig. 3 shows the presence of pits in the surface. A typical pit

can be seen in the AFM image in Fig. 4 which was obtained on an InP electrode that had been subjected to a potential sweep from 0.0 V to 0.7 V. Thus, it is believed that pits such as this penetrate the dense near-surface layer and act as pathways which connect the porous structure with the bulk electrolyte. It is assumed that both the porous layer and the pores through the near-surface layer are filled with electrolyte. This would enable ionic current to flow and electrochemical oxidation of InP to proceed, thus providing a mechanism by which the porous layer can grow.

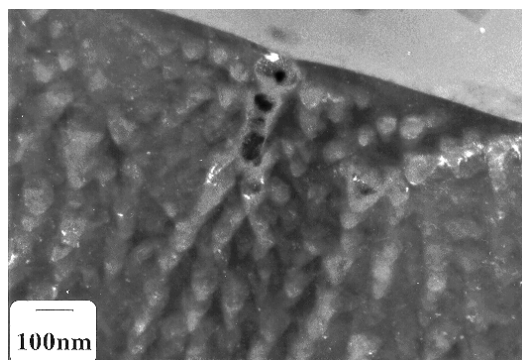


Fig. 3 Dark Field TEM of the porous InP cross-section after a potential sweep from 0.0 V to 0.7 V (SCE) in 5 mol dm⁻³ KOH showing localized degradation and pore propagation from beneath the etch pit formed in the near-surface layer.

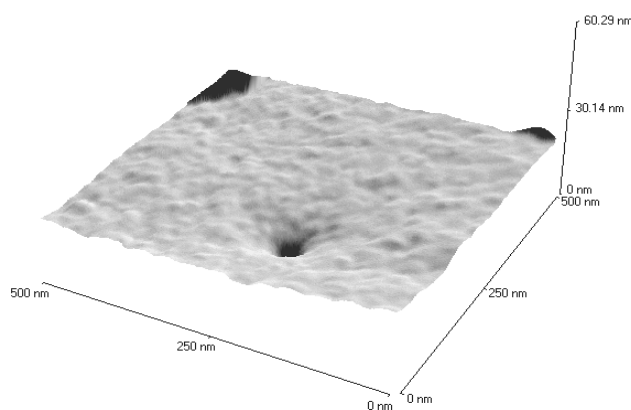


Fig. 4 AFM image obtained after the InP electrode was subjected to a potential sweep from 0.0 V to 0.7 V (SCE) in a 5 mol dm⁻³ KOH electrolyte at a scan rate of 2.5 mV s⁻¹.

Experiments were also carried out at lower concentrations of KOH. Fig. 5 shows linear potential sweeps of InP electrodes in 2 mol dm⁻³ and 3 mol dm⁻³ KOH electrolytes under similar conditions to that outlined in Fig. 1. The potential was scanned at a rate of 2.5 mV s⁻¹ with an initial potential of 0.0 V. The overall response is very similar to what is observed in 5 mol dm⁻³ under similar conditions; anodic current peaks are observed, at 0.43 V in 3 mol dm⁻³ KOH and at 0.52 V in 2 mol dm⁻³ KOH. A shoulder is also observed on the higher potential side of the peak in the 3 mol dm⁻³ case and a fully resolved second peak at 0.7 V in the 2 mol dm⁻³ case.

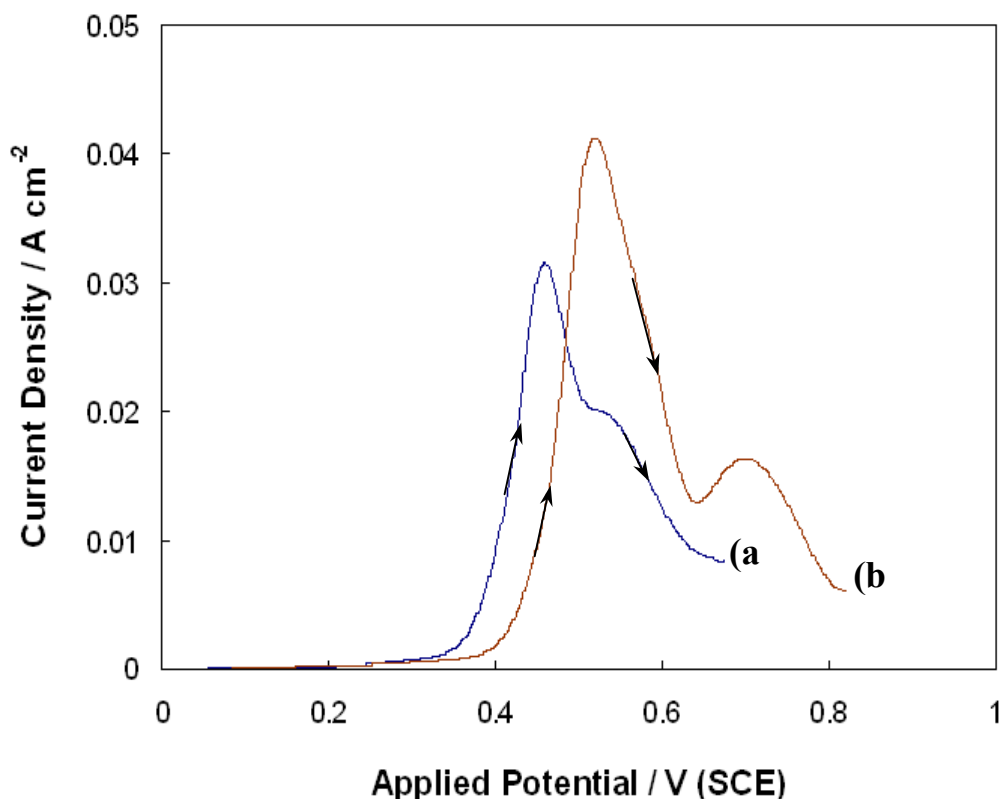


Fig. 5 Linear potential sweeps of InP electrodes in (a) 3 mol dm⁻³ KOH from 0.0 V to 0.675 V and (b) 2 mol dm⁻³ KOH from 0.0 V to 0.825 V. The data was acquired at a scan rate of 2.5 mV s⁻¹.

Cross-sectional TEM confirms that the anodic currents in these electrolytes also correspond to the formation of porous layers. This can be seen in Fig. 6 which shows the cross-sections of electrodes which had been subjected to potential scans from 0.0 V to 0.825 V in 2 mol dm⁻³ KOH and from 0.0 V to 0.675 V in 3 mol dm⁻³ KOH respectively. In each case, a porous layer similar to that obtained in 5 mol dm⁻³ KOH is clearly observed. Again, closer examination reveals the existence of a thin, dense, near-surface layer in each case which is penetrated in places by pores. This can be seen in Fig. 7 for the 2 mol dm⁻³ case.

It is noted however, that porous layer formation is not observed in all concentrations of KOH. Experiments carried out in 1 mol dm⁻³ KOH show anodic current peaks in the cyclic voltammograms but cross-sectional TEM shows that there is no porous layer formation. The results in 1 mol dm⁻³ are discussed in detail elsewhere [22].

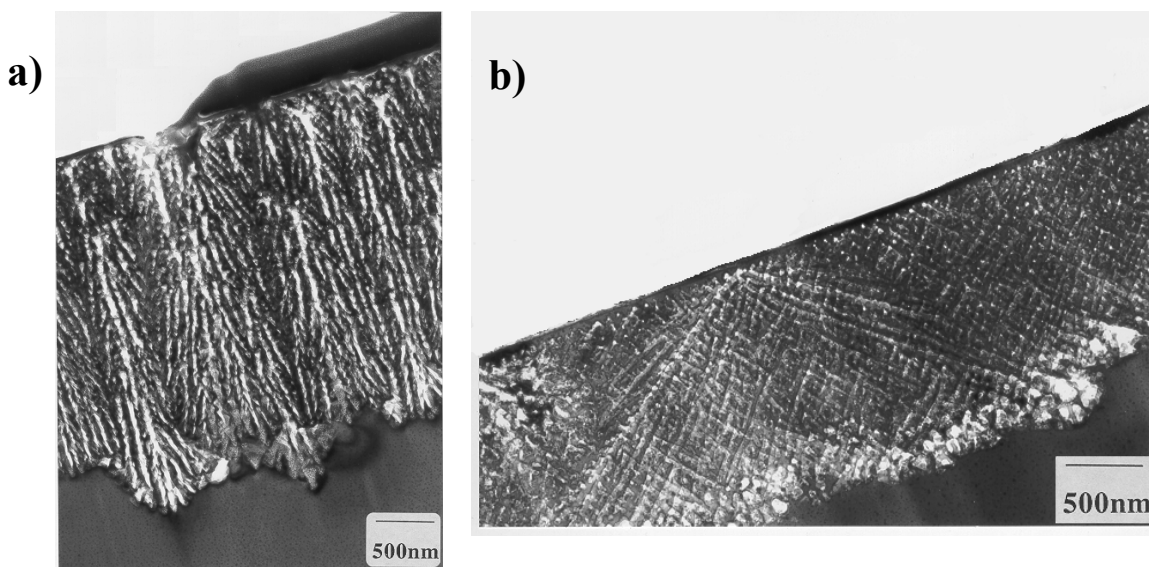


Fig. 6 (a) Bright field TEM of InP after a potential sweep from 0.0 V to 0.825 V (SCE) in 2 mol dm⁻³ KOH (b) Bright field TEM of InP after a potential sweep from 0.0 V to 0.675 V (SCE) in 3 mol dm⁻³ KOH. The potential sweep anodization was scanned at a rate of 2.5 mV s⁻¹. The plane of both micrographs is (110).

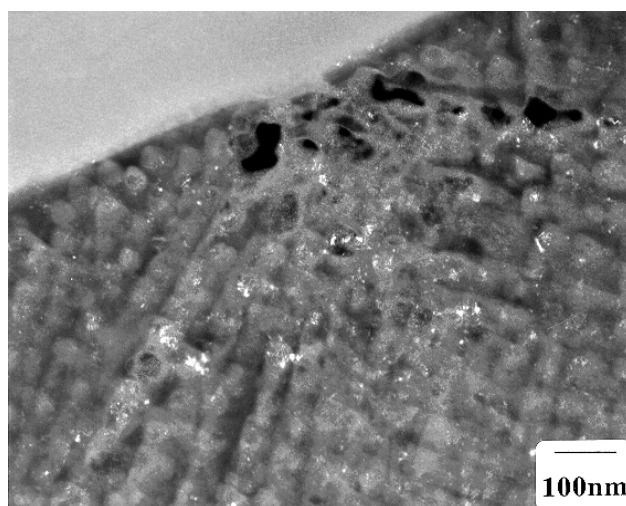


Fig. 7 Dark Field TEM of the porous InP cross-section after a potential sweep from 0.0 V to 0.825 V (SCE) in 2 mol dm⁻³ KOH at a scan rate of 2.5 mV s⁻¹ showing etch pitting of the surface.

The average thickness of the porous layers formed in 2, 3 and 5 mol dm⁻³ KOH after a potential sweep from 0.0 V to 0.825 V, 0.675 V and 0.7 V respectively, was measured from TEM micrographs such as those in Figs. 2 and 6. The values obtained are plotted against the KOH concentration in Fig. 8. The mean pore width was also determined from each of these micrographs. This was done by drawing a series of lines on the micrograph and estimating the width of each pore through which the lines passed. Values estimated in this way are plotted as a function of KOH concentration in Fig. 8. It is clear that both the porous layer thickness and mean pore width decrease significantly with increasing concentration of KOH.

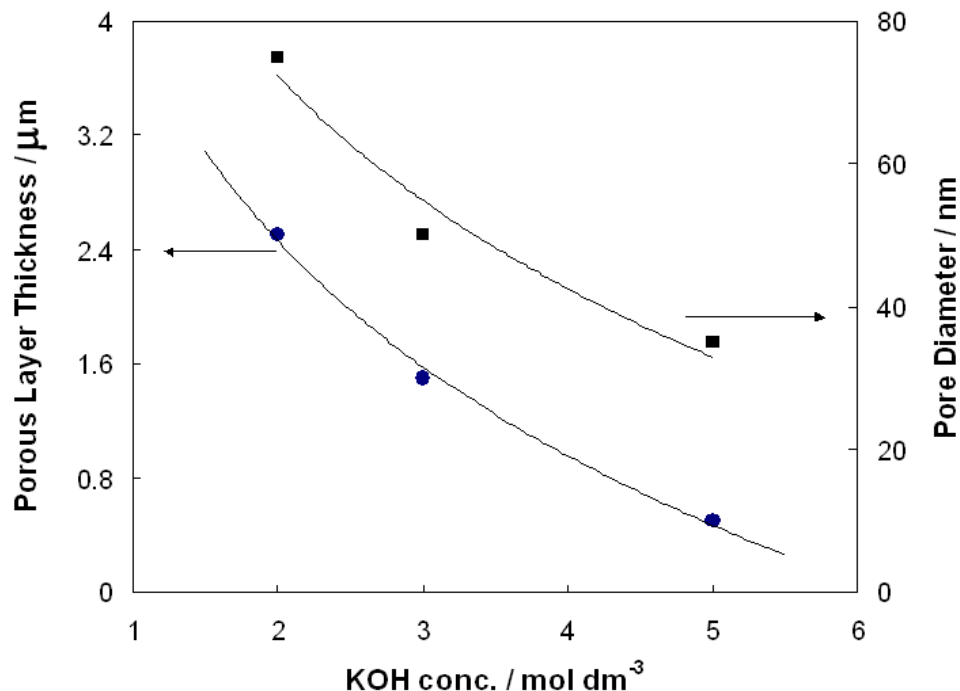


Fig. 8 Plots of the porous layer thickness and mean pore diameter for porous layers formed after a potential sweep at a scan rate of 2.5 mV s^{-1} from 0.0 V to 0.825 V, 0.675 V and 0.7 V (SCE) in 2, 3 and 5 mol dm⁻³ KOH respectively.

Potentiostatic anodization of n-InP electrodes at 0.9 V in 2, 3 and 5 mol dm⁻³ KOH also resulted in the formation of porous InP structures. The porous layers formed potentiostatically were similar to those formed under potential sweep conditions. Typical current-time curves of InP electrodes polarized at 0.9 V in KOH solutions of various concentration are shown in Fig. 9. The current initially increases with time in each case, reaching a peak after 5 – 10 s depending on the KOH concentration, and subsequently decreases. The average thickness of porous layers formed after anodization at 0.9 V for 150 s in 2, 3 and 5 mol dm⁻³ KOH solutions were measured from TEM micrographs. Values of 2.38, 1.68 and 1.18 µm were obtained showing a similar trend to that observed in Fig. 8 for layers formed under potential sweep conditions.

For each of the samples mentioned for which the thickness of the porous layer was measured, the corresponding charge density passed was also estimated. This was done by estimating the integral of current with respect to time. The measured thickness of the porous layer was then plotted against the corresponding charge density. The results are shown in Fig. 10. It is clear that a good fit to a straight line through the origin is obtained. The slope of this line gives a value of $1.10 \text{ µm C}^{-1} \text{ cm}^2$ for the ratio of porous layer thickness to charge density (Fig. 10 (a)). The observation that the porous layer thickness increases linearly with charge density indicates that a relatively constant percentage porosity is maintained.

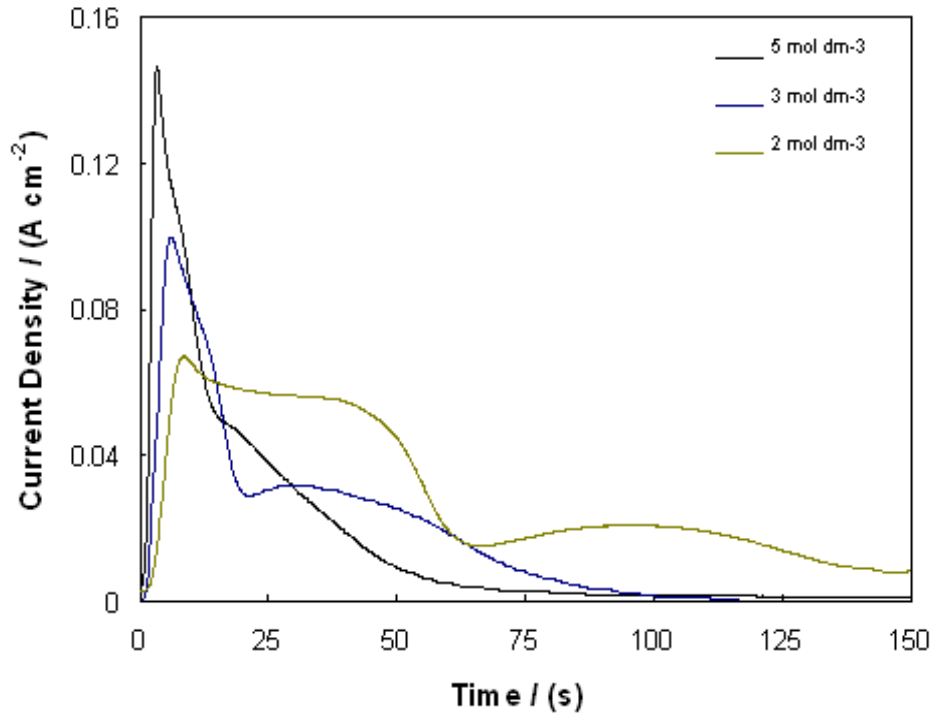


Fig. 9 Current-time curves for InP electrodes anodized at constant potential (0.9 V (SCE)) in 2, 3 and 5 mol dm⁻³ KOH for 150 seconds.

A theoretical value for the ratio of layer thickness to charge density passed was also estimated. Using Faraday's law, the ratio of the thickness d of InP oxidized to the charge density Q is given by the equation

$$\frac{d}{Q} = \frac{V_{M(\text{InP})}}{nF} \quad (1)$$

where $V_{M(\text{InP})}$ is the molar volume of InP, n is the number of electrons per formula unit of InP and F is the Faraday constant. Using a value of 30.31 cm³ mol⁻¹ for $V_{M(\text{InP})}$ and assuming $n = 8$, a theoretical value of 0.393 $\mu\text{m C}^{-1} \text{cm}^2$ is estimated from Eqn. (1) for d/Q , the ratio of layer thickness to charge density for complete removal of InP. This theoretical ratio is represented by line (b) in Fig. 10. As indicated above, the slope of line (a) provides an estimate of 1.10 $\mu\text{m C}^{-1} \text{cm}^2$ for the corresponding ratio d_e/Q of experimental porous layer thickness d_e to charge density. The ratio of these estimates of d/Q and d_e/Q gives a value of $r = d/d_e = 0.357$, *i.e.* the estimated thickness of a compact InP layer is a fraction $r = 0.357$ of the corresponding as-measured porous layer thickness. Using the estimated value of $r = 0.357$ we obtain an estimate of approximately 65% or the porosity of the porous InP layers.

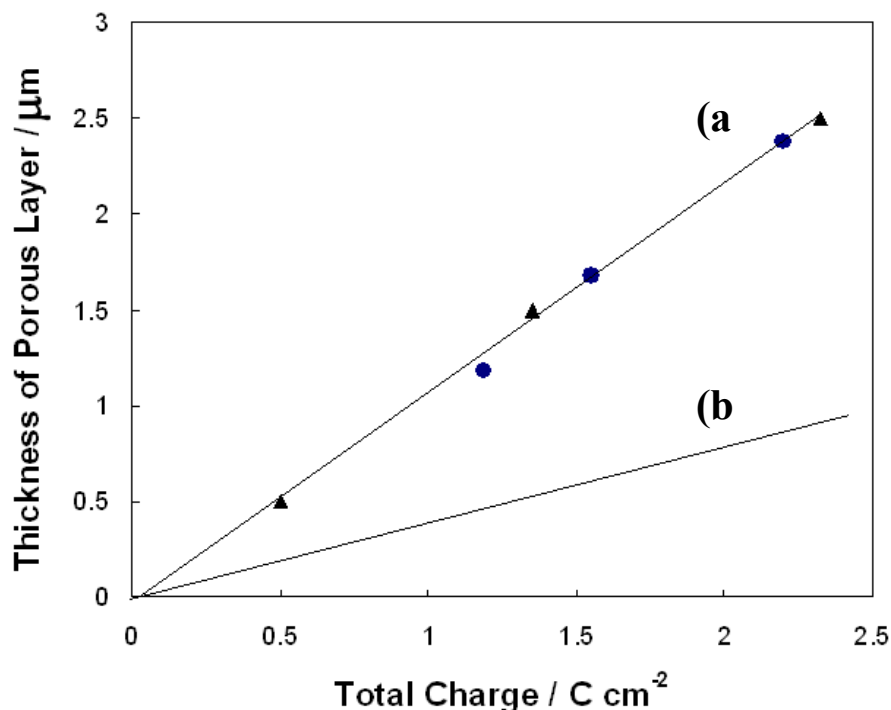


Fig. 10 Plot of porous layer thickness for samples anodized at constant potential (●) and after potential sweep (▲) as a function of the charge passed. (-) Theoretical thickness of InP removed.

Details of the mechanism of growth of porous layers are under investigation. The evidence presented here strongly suggests that the porous layer structure arises from the penetration of pits into the surface at particular points and pore propagation within the InP originating at these points. Presumably, the pores are filled with electrolyte, pore growth occurs at pore tips and the electrolyte within the porous structure is connected to the bulk electrolyte through the surface pits which penetrate the dense near-surface layer. Preliminary evidence suggests that pore growth may occur only along the $\langle 100 \rangle$ direction. The origin of the dense near-surface layer has not been fully explained but it is suggested that it may arise from carrier depletion in the semiconductor. The detailed electrochemistry also requires investigation.

CONCLUSIONS

Electrochemical anodization of n-InP in relatively high concentrations of KOH solutions in dark conditions results in the formation of highly porous InP layers. Both potentiodynamic and potentiostatic anodization results in porous layer formation. Selective dissolution of the electrode surface occurs and the pores appear to propagate along the $\langle 100 \rangle$ crystallographic directions from beneath the pits. The thickness of the porous layer and the mean pore diameter are noted to decrease with increasing KOH concentration both under potentiostatic and potentiodynamic anodization. For all porous layer formed in KOH, a relatively constant percentage porosity of 65% is maintained. Details of the mechanism of porous layer growth are still being investigated.

REFERENCES

- [1] L.T. Canham, *Appl. Phys. Lett.*, **57**, 1046 (1990)
- [2] H. Föll, *Appl. Phys. A*, **53**, 8 (1991)
- [3] T. Holec, T. Chvojka, I. Jelínek, J. Jindřich, I. Němec, I. Pelant, J. Valenta and J. Dian, *Mater. Sci. Eng. C*, **19**, 251 (2002)
- [4] R.J. Martín-Palma, J.M. Martínez-Duart, L. Li and R.A. Levy, *Mater. Sci. Eng. C*, **19**, 359 (2002)
- [5] A. Matoussi, T. Boufaden, A. Missaoui, S. Guermazi, B. Bessaïs, Y. Mlik and B. El Jani, *Microelectronics Journal*, **32**, 995 (2001)
- [6] A. Jain, S. Rogojevic, S. Ponoth, N. Agarwal, I. Matthew, W.N. Gill, P. Persans, M. Tomozawa, J.L. Plawsky and E. Simonyi, *Thin Solid Films*, **398**, 513 (2001)
- [7] N.E. Chayen, E. Saridakis, R. El-Bahar, Y. Nemirovsky, *J. Molec. Biol.*, **312**, 591 (2001)
- [8] S. Langa, I. M. Tiginyanu, J. Carstensen, M. Christopherson and H. Föll, *Electrochem. Solid-State Lett.*, **3**, 514 (2000)
- [9] S. Langa, J. Carstensen, I.M. Tiginyanu, M. Christopherson and H. Föll, *Electrochem. Solid-State Lett.*, **4**, G50 (2001)
- [10] F.M. Ross, G. Oskam, P.C. Searson, J.M. Macaulay and J.A. Liddle, *Philos. Mag. A*, **75**, 2 (1997)
- [11] E. Harvey, C. O'Dwyer, T. Melly, D.N. Buckley, V.J. Cunnane, D. Sutton, S.B. Newcomb and S.N.G. Chu, in *Proceedings of the 35th State-of-the-Art Program on Compound Semiconductors*, P.C. Chang, S.N.G. Chu, and D.N. Buckley, Editors, PV 2001-2, p. 87, The Electrochemical Society, Proceedings Series, Pennington, NJ (2001)
- [12] M.M. Faktor, D.G. Fiddymment and M.R. Taylor, *J. Electrochem. Soc.*, **122**, 1566 (1975)
- [13] D.J. Lockwood, P. Schmuki, H.J. Labbé, J.W. Fraser, *Physics E*, **4**, 102 (1999)
- [14] X.G. Zhang, S.D. Collins, R.L. Smith, *J. Electrochem. Soc.*, **136**, 1561 (1989)
- [15] J.S. Shor, I. Grimberg, B.-Z. Weiss and A.D. Kurtz, *Appl. Phys. Lett.*, **62**, 2836 (1993)
- [16] A. Uhler, Jr., *Bell System Tech. J.*, **35**, 333 (1956)
- [17] P. Schmuki, J. Fraser, C.M. Vitus, M.J. Graham, H.S. Isaacs, *J. Electrochem. Soc.*, **143**, 3316 (1996)
- [18] P. Schmuki, D.J. Lockwood, J. Fraser, M.J. Graham, H.S. Isaacs, *Mater. Res. Soc. Symp. Proc.*, **431**, 439 (1996)
- [19] M. Christopherson, J. Carstensen, A. Feuerhake and H. Föll, *Mater. Sci. Eng. B*, **69**, 70, 194 (2000)
- [20] S. Rönnebeck, J. Carstensen, S. Ottow and H. Föll, *Electrochem. Solid-State Lett.*, **2**, 126 (1999)
- [21] P. Schmuki, L.E. Erickson, D.J. Lockwood, J.W. Fraser, G. Champion, H.J. Labbé, *Appl. Phys. Lett.*, **72**, 1039 (1998)
- [22] C. O'Dwyer, D.N. Buckley, V.J. Cunnane, D. Sutton, M. Serantoni and S.B. Newcomb, in *Proceedings of the 37th State-of-the-Art Program on Compound Semiconductors*, This Volume, The Electrochemical Society, Proceedings Series, Pennington, NJ (2001)

